Evolution of a small phage protein overcomes antiphage defense in *Enterococcus faecalis*

Cydney N. Johnson*[1,2], Nathan P. Bullen*[3,4], Shelby E. Andersen[1], Garima Arya[1], Sonia R. Marotta[3,4], John C. Whitney[3,4,#], Breck A. Duerkop[1,#]

*Authors contributed equally to this work

[1]Department of Immunology and Microbiology, University of Colorado School – Anschutz Medical Campus, School of Medicine, Aurora, CO, USA, 80045

[2]Department of Host-Microbe Interactions, St. Jude Children's Research Hospital, Memphis, TN, USA, 38105

[3]Department of Biochemistry and Biomedical Sciences, McMaster University, Hamilton, ON, Canada, L8S 4L8

[4]Michael DeGroote Institute for Infectious Disease Research, McMaster University, Hamilton, ON, Canada

[#]Correspondence: Breck A. Duerkop, breck.duerkop@cuanschutz.edu or John C. Whitney, jwhitney@mcmaster.ca

Key words: Bacteriophages, *Enterococcus faecalis*, plasmid, antiphage, type IV restriction enzyme

ABSTRACT

The prevalence of multidrug resistant (MDR) bacterial infections continues to rise as the development of new antibiotics needed to combat these infections remains stagnant. MDR enterococci, which are a common cause of hospital-acquired infections, are emerging as one of the major contributors to this crisis. A potential therapeutic approach for combating MDR enterococci is bacteriophage (phage) therapy, which entails the use of lytic viruses to infect and kill pathogenic bacteria. While phages that lyse some strains of MDR enterococci have been identified, other strains display high levels of phage resistance and the mechanisms underlying this resistance are unknown. Here, we use a CRISPR interference (CRISPRi) screen to identify a genetic locus found on a mobilizable plasmid from vancomycin-resistant *Enterococcus faecalis* involved in phage resistance. This locus encodes a putative serine recombinase followed by a Type IV restriction enzyme (TIV-RE) and we show that this enzyme is sufficient to restrict the replication of the lytic phage in *E. faecalis*. We further find that phages can evolve to overcome restriction by acquiring a missense mutation in a novel TIV-RE inhibitor protein encoded by many enterococcal phages. We show that this inhibitor, which we have named anti-restriction-factor A (*arfA*), directly binds to and inactivates diverse TIV-REs. Overall, our findings significantly advance our understanding of phage defense in drug-resistant *E. faecalis* and provide mechanistic insight into how phages can evolve to overcome antiphage defense systems.

INTRODUCTION

While typically members of the gut microbiota of humans and other animals, the enterococci are Gram-positive bacteria that can cause life-threatening disease following antibiotic-mediated dysbiosis (1, 2). During antibiotic treatment, multidrug-resistant (MDR) *Enterococcus faecalis* can outgrow antibiotic-sensitive members of the microbiota and this increases the likelihood that MDR *E. faecalis* will breach the intestinal barrier and enter the bloodstream leading to sepsis (1, 2). These MDR infections are difficult to treat due to limited antibiotic options and consequently, bacteriophages or phages (viruses that infect bacteria) are increasingly being considered as a therapeutic option as the frequency of MDR infections continues to rise (3-5). Phage therapy offers advantages over traditional antibiotic therapy because phages exhibit strain-level specificity, which reduces off-target bacterial killing, they are self-limiting following the exhaustion of their bacterial host, and their abundance in nature implies that a phage specific to a target bacterium can usually be identified (6-10).

As is the case with the emergence of antimicrobial resistance, exposure of bacteria to phages also imposes a strong selective pressure that leads to the evolution or acquisition of mechanisms to resist infection. Recent studies have shown that bacteria have evolved diverse antiphage defense systems to prevent successful phage infection (11-13). These systems are often concentrated in bacterial genomes within so-called “defense-islands”, which are characterized by the clustering of genes encoding two or more defense systems and are typically carried on mobile genetic elements, including integrative and conjugative elements, plasmids, transposons, and temperate phages (14-16). This capacity to mobilize and spread between bacterial species represents a robust pan-genomic immune system that contributes to the rapid evolution of resistance to phage infection and constitutes a significant challenge to the effective application of phage therapy.

Antiphage defenses utilize a variety of mechanisms to overcome phage infection. These include nucleic acid interference systems in which host proteins epigenetically label nucleobases and/or the phosphate backbone to distinguish host self-DNA from phage DNA, RNA-based adaptive nucleic acid targeting systems such as CRISPR-Cas (17-22), toxin-antitoxin and other phage interference systems that stop phage replication and spread (23-27), chemical defenses that can restrict phage infection (28), and phage receptor alteration which abrogates the ability of phages to interact with the bacterial cell surface (29-33). Phages have evolved counter-defenses to antiphage defense systems that include modification of tail proteins for bacterial cell recognition, DNA modification to avoid restriction systems, and phage-encoded proteins that interfere with antiphage defenses (34-38). Compared to bacterial antiphage defense systems, the breadth of phage-encoded proteins that support counter-defenses and the mechanisms that drive their evolution are poorly understood. Thus, prior to phages being widely used as therapeutics for MDR bacterial infections, a detailed understanding of the mechanisms by which bacteria subvert phage infection and, conversely, how phages overcome these mechanisms is needed.

In this study, we sought to understand why some MDR strains of *E. faecalis* are susceptible to infection by virulent enterococcal phages whereas others exhibit complete resistance(39). By conducting a CRISPR interference (CRISPRi) screen on one such resistant strain, we pinpoint its mechanism of resistance to a two-gene locus residing on a pheromone responsive plasmid that inhibits infection of the enterococcal phage phi47. Further analysis revealed that resistance to phi47 infection is solely conferred by the activity of one of these genes, EF_B0059, encoding a putative type IV restriction enzyme (TIV-RE). We isolated phages that are resistant to restriction by EF_B0059 and in doing so discovered that the *orf65* gene of phi47 encodes a small protein that can evolve to not only bind and inactivate EF_B0059 but also other highly divergent type IV restriction enzymes. From this, we posit that Orf65 is a

rapidly evolving and broadly acting anti-TIV-RE protein. Overall, our data demonstrate that *E. faecalis* utilizes a mobilizable antiphage system to resist phage infection, and that phages escape this restriction through a coevolving small open reading frame found in enterococcal and related phages.

RESULTS

The pheromone responsive plasmid pTEF2 is sufficient to inhibit phage infection

In our attempts to understand the mechanisms underlying phage-host interactions in MDR enterococci, we previously observed that the lytic *E. faecalis* phage phi47 can infect *E. faecalis* strain SF28073 but not the closely related strain V583 (39). Curiously, phi47 readily adsorbs to both SF28073 and V583, indicating that this resistance cannot be attributed to differences in the cell surface of these strains preventing phage binding (39). From this, we hypothesized that *E. faecalis* V583 may encode one or more antiphage defense systems that restrict the replication of phi47.

A comparison of the *E. faecalis* SF28073 and V583 genomes revealed that their core genomes are very similar, sharing nearly 90% sequence identity (Fig. S1A). However, sequence comparison of the three natural plasmids carried by these strains showed that the plasmids of V583 (pTEF1, pTEF2, pTEF3) differed significantly from that of SF28073 (pSF1, pSF2, pSF3) (Fig S1B). Based on these observations, we reasoned that one or more plasmid(s) of V583 may be responsible for resistance to phi47 infection. To explore this idea, we infected *E. faecalis* V19, a plasmid-cured derivative of V583, with phi47 (40, 41). Unlike V583, V19 supports robust replication of phi47 indicating that one or more of the three V583 plasmids confers resistance to phi47 (Fig. 1A). Of these three plasmids, pTEF1 and pTEF2 are pheromone responsive plasmids (PRPs). PRPs mobilize through conjugation upon the recognition of a peptide

pheromone signal produced by plasmid-free cells (42). In contrast to pTEF1 and pTEF2, pTEF3 is a comparatively small, non-mobilizable plasmid (43). Given that plasmid mobilization likely disseminates antiphage defenses, we focused our efforts on pTEF1 and pTEF2.

To determine which of the *E. faecalis* V583 mobilizable plasmids mediates resistance to phi47, we conjugated pTEF1 and pTEF2 into the phi47 susceptible *E. faecalis* V19 strain. Subsequent infections with phi47 showed pTEF1 had no effect on the ability of phi47 to replicate in V19, whereas the carriage of pTEF2 entirely restricted phi47 replication (Fig. 1A). This pTEF2-mediated resistance to phi47 is independent of the *E. faecalis* strain background as the mobilization of pTEF2 into *E. faecalis* JH2-2, which shares 87% of its genome at a nucleotide identity of 99% or greater with V583 (44), was sufficient to prevent replication of phi47 (Fig. 1A). To confirm that no infectious phages were being released from pTEF2-containing cells, we also measured total infectious phi47 production during infection (Fig. 1B). While the strains V19 and SF28073 support the production of infectious phi47 particles, V19 pTEF2 grown in the presence of phi47 did not show an increase in recoverable phages over time.

Some antiphage defense systems are predicted to function through a mechanism termed abortive infection, whereby the activation of the antiphage system stops the spread of virus at the expense of the viability of the bacterial host. Abortive infection systems are proposed to be widespread among bacteria, however, there is debate as to whether they kill the bacterial cell or halt its metabolism leading to a persister state that cannot support phage replication (45). Such population-level resistance can be measured by infecting bacteria with phage at high multiplicities of infection (MOI) because this results in the complete collapse of the bacterial culture. In contrast, some defense systems confer individual-level resistance to phage, often by directly targeting phage replication processes during early infection. In these instances, bacterial growth upon phage infection is comparable at low and high MOIs. To

determine if phi47 resistance is due to abortive infection, we measured the optical density (OD_{600}) of *E. faecalis* cultures during infection by phi47 at an MOI of 10 (Fig. S2A). In doing so, we observed that V19 pTEF2 cells continued to grow during phi47 infection at a similar rate to that of uninfected V19 pTEF2. Thus, the pTEF2 antiphage defense is not mediated by abortive infection, but instead provides direct immunity to phi47. Additionally, we confirmed that phi47 adsorbed equally to the cell surface of both V19 and V19 pTEF2 compared to V583 (Fig. S2B). Taken together, our data suggests that the pheromone responsive plasmid pTEF2 encodes an antiphage defense system that does not function by abortive infection or by preventing phage adsorption.

A two-gene operon encoded on pTEF2 is responsible for phage restriction

We next determined which gene(s) on pTEF2 were responsible for the restriction of phi47. Of the 62 open reading frames (ORFs) encoded by pTEF2, approximately half are predicted to be involved in the maintenance and conjugation of the plasmid. Furthermore, more than half of the genes on pTEF2 share 95-97% sequence identity to another *E. faecalis* PRP, pCF10, which, unlike pTEF2, does not confer resistance to phi47 when conjugated into V19 (Fig. 2A and 2B). Comparing the sequences of pTEF2 and pCF10 revealed that pTEF2 encodes a unique 15 kb region encompassing 18 ORFs not present in pCF10 (EF_B0048 to EF_B0065). We reasoned that the gene(s) involved in phi47 restriction were therefore likely encoded by one or more these 18 ORFs.

To test this prediction, we performed a CRISPR interference (CRISPRi) gene knockdown screen in *E. faecalis* V19 pTEF2. CRISPRi uses a catalytically inactive Cas9 (dCas9) that binds to target DNA sequences when directed by complementary small guide RNAs (sgRNAs), resulting in transcriptional repression of target genes (46). We designed

169 sgRNAs to target each of the 18 ORFs unique to pTEF2 and transformed these into V19 pTEF2
170 cells to selectively knock down target gene expression. The relative viability of the resulting
171 transformants was then measured in the presence or absence of phi47 (Fig. 2C). Strikingly,
172 under these experimental conditions, the sgRNA-dependent repression of either EF_B0058 or
173 EF_B0059 resulted in a significant decrease in cell viability when compared to V19 pTEF2 or
174 V19 transformed with a control sgRNA (sgRNA-GFP). To validate the findings of our screen, we
175 generated single gene knock outs in pTEF2 of either EF_B0058 or EF_B0059 in both V583 and
176 V19 (Fig. 2D and 2E). Subsequent infections with phi47 in these strains revealed that the
177 deletion of EF_B0058 did not restore the ability of phi47 to replicate in V583 or V19 whereas
178 deletion of EF_B0059 did. This result indicates that EF_B0059 alone confers resistance to phi47
179 infection. A closer examination of the genetic context of EF_B0058 and EF_B0059 found that
180 these genes are encoded in tandem and are separated by a small intergenic region (54 base
181 pairs), suggesting that they may be encoded on the same mRNA (Fig. 2F). To test this
182 prediction, we performed reverse-transcription PCR to generate cDNA from total RNA purified
183 from *E. faecalis* V19 with and without pTEF2. PCR reactions using this cDNA as a template and
184 primers that span the intergenic region between EF_B0059 and EF_B0058 revealed that
185 EF_B0058 and EF_B0059 exist on the same mRNA (Fig. 2G). From this finding, we concluded
186 that the sgRNA targeting EF_B0058 likely also disrupts the expression of downstream
187 EF_B0059, resulting in a reduced capacity to restrict phi47.

188 Bioinformatic analyses, including the generation of a high-confidence Alphafold2 model
189 of EF_B0059, predict that this antiphage protein belongs to the GmrSD-like type IV modification-
190 dependent restriction enzyme family (Fig. S3A and S3B). This family of proteins is defined by N-
191 terminal DUF262 and C-terminal DUF1524 domains connected by a small α-helical domain of
192 variable length (Fig. S3A) (47). DUF262 domains function as NTPases and contain a conserved
193 (I/V)DGQQR motif that forms a nucleotide binding pocket whereas DUF1524 domains are

structurally similar to HNH endonucleases and contain a conserved EHxxP catalytic motif found in members of the broad His-Me finger endonuclease superfamily (47, 48). EF_B0059 possesses an intact DUF262 VDGQQR motif but has a glutamate in place of the conserved proline in its DUF1524 EHxxP motif (Fig. S3A). The precise molecular details describing how these two domains coordinate DNA substrate recognition and cleavage are not yet understood, however, NTP hydrolysis by the N-terminal DUF262 has been shown to drive conformational changes that activate DUF1524's nuclease activity resulting in DNA cleavage (47, 49). Moreover, these enzymes have been shown to target diverse types of modified DNA, in particular DNA containing modified cytosine bases (50, 51). Given this precedent, we expressed EF_B0059 in an *E. coli* K-12 derivative that contains 5-methylcytosine in its DNA under the assumption that overexpression of this putative TIV-RE would likely target the DNA of an evolutionary distant bacterial species as long as its DNA contained the appropriate modification. Indeed, we found that the heterologous expression of EF_B0059 is extremely toxic to *E. coli* (Fig. 2H). Importantly, this growth inhibition is dependent on both the NTPase and nuclease activities of EF_B0059 as mutations in the conserved catalytic sites of either domain were non-toxic, despite each variant expressing to higher levels than the wild-type protein (Fig. 2I). Combined, these data suggest that EF_B0059 is a TIV-RE that targets modified DNA.

pTEF2-mediated resistance is overcome by a phage-encoded protein

Because phages are entirely dependent on their host for replication, they are under strong selective pressure to evolve ways to evade their host defense systems. Thus, we next asked if phi47 can evolve to overcome EF_B0059-dependent restriction. To determine this, we infected phi47-resistant *E. faecalis* V19 pTEF2 with more than 1000-fold excess phi47 and were able to isolate nine escape phage plaques. Subsequent infections with the phages isolated from each of these plaques confirmed that they replicate equally on V19 and V19 pTEF2 (Fig. S4A).

Intriguingly, whole genome sequencing of these phages found that they all harbor a single point mutation in the small open reading frame, *orf65*, that results in a nonsynonymous mutation at amino acid 32 from leucine to phenylalanine (Fig 3A). Mutations in phage genomes often arise to prevent DNA targeting defense systems from recognizing phage DNA substrate (52, 53). However, the conserved nonsynonymous mutation identified in all phages that overcame EF_B0059 restriction suggested that the gene product of *Orf65* is instead responsible for evading EF_B0059 activity. To test this, we infected *E. faecalis* V19 pTEF2 cells ectopically expressing either the wildtype or evolved Orf65 ($Orf65^{L32F}$) with phi47 (Fig 3B). These results confirmed that the evolved $Orf65^{L32F}$, but not the native protein, confers resistance to EF_B0059-dependent restriction.

To understand how this phage protein prevents restriction by EF_B0059 we next generated a high confidence Alphafold2 model of $Orf65^{L32F}$ (Fig. 3C and S4B) (54-56). Orf65 is predicted to be a small protein consisting of two globular domains connected by a short linker. Structural alignments to proteins of known structure identified minimal similarity to characterized proteins with the exception of an N-terminal SH3-like domain (57). SH3 domains are found in diverse protein families across all domains of life and are generally involved in protein-protein interactions (58, 59). From this predicted structure, we also noted that Orf65 encodes an unusually high number of acidic residues (21.3%) that are found on the surface of the protein resulting in a large electronegative surface potential (Fig. 3D). This degree of surface electronegativity is reminiscent of the anti-restriction protein Ocr of phage T7. Ocr is a negatively charged protein (29% acidic amino acids) whose structure mimics B-DNA, which facilitates its binding and inactivation of Type I restriction enzymes by competing with their DNA substrates (60, 61) Although the predicted structure of $Orf65^{L32F}$ does not resemble Ocr or mimic the structure of B-DNA, its similar electronegative surface properties and the presence of

an SH3 domain likely involved in protein-protein interactions led us to hypothesize that it functions as a direct inhibitor of EF_B0059.

If our hypothesis is correct, we would expect Orf65^{L32F} to inhibit the activity of EF_B0059 in the absence of any additional phi47- or *E. faecalis*-encoded factors. To test this, we heterologously co-expressed EF_B0059 with either the wildtype Orf65 or the Orf65^{L32F} variant in *E. coli*. Consistent with our phi47 infection data, expression of the Orf65^{L32F} variant but not the wildtype protein restored *E. coli* growth when co-expressed with the normally toxic EF_B0059 (Fig. 3E and 3F). Next, to determine if the observed Orf65^{L32F} inactivation is dependent on a physical interaction with EF_B0059, we immunoprecipitated FLAG-tagged EF_B0059 from cells co-expressing either VSV-G-tagged Orf65 or Orf65^{L32F}. Western blotting of the precipitated fractions showed that wild-type EF_B0059 co-precipitates with a small amount of Orf65, which our co-expression data indicate is insufficient to alleviate the toxic effects of EF_B0059 on *E. coli*. Notably, however, we found that VSV-G tagged Orf65^{L32F} was substantially more enriched than the wildtype protein upon immunoprecipitation suggesting that the inhibitory properties of this variant are due to enhanced binding to EF_B0059 (Fig 3G). Importantly, in the absence of EF_B0059, neither Orf65 nor Orf65^{L32F} precipitate with α-FLAG conjugated agarose, confirming that the observed interactions are specific (Fig. S4C). Overall, these data suggest that while the wildtype Orf65 interacts with EF_B0059, the L32F mutation likely increases its binding affinity. Interestingly, mutation of leucine 32 to alanine or to other aromatic residues does not result in Orf65 variants capable of binding and inactivating EF_B0059, suggesting that the presence of the phenylalanine residue specifically stabilizes the Orf65^{L32F}-EF_B0059 complex (Fig S4D and S4E). Taken together, our data reveal that phi47 encodes a small, negatively charged protein that can evolve to inhibit the activity of EF_B0059. Interaction studies indicate that this inhibition is mediated by the direct binding of Orf65 to EF_B0059 and that this interaction is strongly influenced by a phenylalanine substitution at position 32 of Orf65.

Orf65 represents a family of phage-encoded anti-type IV restriction enzymes.

The isolation of phage mutants that can infect phi47-resistant *E. faecalis* pTEF2 revealed that phi47 can evolve to overcome the restriction activity of the TIV-RE, EF_B0059. It achieves this through a single point mutation in the small protein Orf65, which promotes the binding and inactivation of EF_B0059. While wildtype Orf65 also binds EF_B0059, it does not display the same inhibitory effect. Intriguingly, sequence comparisons between Orf65 homologues from the genomes of closely related enterococcal phages found that phenylalanine naturally occurs at position 32 in the *E. faecalis* phage SDS2, indicating that phages related to phi47 may have previously evolved to overcome restriction by EF_B0059 and/or close homologs of this TIV-RE (Fig. 4A). This observation suggests that the L32F substitution we isolated may be representative of an ongoing evolutionary arms race between phages that encode *Orf65* and the hosts that use EF_B0059 and related proteins to restrict their growth.

To probe this idea experimentally, we first asked if Orf65 from phage SDS2, which contains 84% sequence identity to Orf65 from phi47, can inactivate EF_B0059. However, owing to factors unrelated to the activity of EF_B0059, we found that phage SDS2 was unable to infect the phi47-susceptible strain V19 or the phi47-resistant strain V583. Further, we found that over-expression the SDS2 Orf65 homolog is toxic to *E. coli* thereby precluding us from testing if it can inactivate EF_B0059 in this heterologous expression system (Fig. S5A). However, if EF_B0059 and Orf65 are co-evolving as an effector-inhibitor pair, we reasoned that wildtype Orf65 protein is likely already effective at inhibiting an EF_B0059-related restriction enzyme without requiring any amino acid substitutions. To test this hypothesis, we searched a database of human intestinal bacterial isolates using the EF_B0059 sequence to identify candidate homologues. As we expected, genes from enterococci and related bacteria were enriched in this context. From this search, we identified two predicted TIV-REs that included GC1503 from *Clostridium*

sporogenes, and GC874 from *Leuconostoc mesenteroides*. These homologues share 33% sequence identity to each other and only 21% sequence identity to EF_B0059. Despite this relatively low sequence identity, comparison of the Alphafold2-predicted structures of these homologues with that of EF_B0059 shows that these enzymes are structurally very similar (Fig. S6). However, while each retains the conserved VDGQQR nucleotide binding motif of the DUF262 domain, GC1503 encodes the canonical proline in DUF1524's EHxxP nuclease motif, whereas GC874 encodes a serine at this site.

The heterologous expression of these proteins in *E. coli* revealed that like EF_B0059, GC1503 is toxic to *E. coli*, whereas GC874 is not, suggesting GC1503 functions more similarly to EF_B0059 (Fig. S5B). Using this same assay, we asked if the co-expression of GC1503 with either Orf65 or Orf65^{L32F} restores *E. coli* growth. Remarkably, and in contrast to EF_B0059, we found that both wildtype and the L32F mutant of Orf65 were able to restore *E. coli* viability (Fig. 4B and S5C). Moreover, co-immunoprecipitation experiments using FLAG-tagged GC1503 revealed that wildtype Orf65 forms a complex with GC1503 that is comparable in abundance to that of the L32F mutant containing complex (Fig. 4C). Intriguingly, these data indicate that although position 32 of Orf65 from phi47 is essential to stabilize its interaction with EF_B0059, it has no effect on its ability to inhibit GC1503. Indeed, each of the L32 variants (Trp, Tyr, and Ala) that we originally tested with EF_B0059 and were found to be non-protective are still protective against GC1503 activity (Fig. S5D). Therefore, the molecular mechanism of Orf65 binding to EF_B0059 homologous proteins is likely multivalent, arising from multiple protein-protein contacts whose significance at the individual amino acid level differs depending on the TIV-RE in question.

We next sought to determine how generalizable the inhibitory activity of Orf65 is to more divergent TIV-REs. To this end, we tested if the expression of Orf65 or its L32F variant interferes with the activity of BrxU, a recently characterized TIV-RE from the Gram-negative

bacterium *Escherichia fergusonii* that shares only 13% sequence identity with EF_B0059 (51). Remarkably, expression of either Orf65 or Orf65^{L32F} interfered with the ability of BrxU to restrict the infection of *E. coli* by a waste-water isolated coliphages with wildtype Orf65 exhibiting a greater inhibitory effect than Orf65^{L32F} (Fig. 4D). In accordance with these data, co-immunoprecipitation experiments with FLAG-tagged BrxU found that both wildtype and Orf65^{L32F} interact with BrxU, however, in contrast to EF_B0059, the L32F mutation had a negative effect on the capacity of Orf65 to bind BrxU (Fig. 4E).

Together, our data strongly supports the conclusion that Orf65 of phi47 encodes a novel anti-TIV-RE factor. The results of our *E. coli* toxicity data in combination with our phage evolution experiments suggest that these phage proteins retain the ability to bind and inactivate diverse TIV-REs, but can readily evolve to become efficient inhibitors upon exposure to a particular TIV-RE. Due to this newly defined role in overcoming anti-phage defense, we propose to name Orf65 Anti-type-IV-restriction factor A (ArfA).

DISCUSSION

The need for alternative therapies to combat MDR bacterial infections has renewed interest in understanding how bacteria defend against phage infection. The majority of this research has prioritized the discovery and characterization of antiphage defense systems in model bacteria such as *E. coli* and *Bacillus subtilis,* with minimal focus on systems found in medically relevant and less-genetically tractable bacteria (20, 21, 26, 62, 63). Moving forward there is a need to prioritize the characterization of such systems in bacteria that are responsible for MDR infections that will ultimately be the targets of phage therapy. Here, we identify a previously unknown TIV-RE encoded on the mobilizable enterococcal plasmid pTEF2. This protein, EF_B0059, limits phage replication without causing death of the infected cell. phi47

phages can overcome this restriction via a single point mutation of leucine to phenylalanine (L32F) in the previously uncharacterized protein Orf65, which herein has been renamed ArfA. This mutation results in a gain-of-function inhibitory protein-protein interaction between ArfA and EF_B0059. Intriguingly, EF_B0059 neutralization strictly depends on a phenylalanine at position 32 and inhibition is lost when other aromatic amino acids are substituted in this position. However, wildtype ArfA binds and neutralizes other TIV-REs, suggesting that ArfA represents a broadly active inhibitor of TIV-REs that undergoes adaptive evolution.

Protein-based antirestriction mechanisms have been described. One well-studied inhibitor is the Ocr protein of the *Escherichia coli* phage T7. Ocr inhibits type I restriction enzymes by mimicking the shape and charge of B-DNA to bind restriction enzymes with picomolar affinity, thereby blocking phage DNA recognition and cleavage (20, 61, 64-66). Other characterized antirestriction proteins include the DNA binding proteins DarA and DarB of *E. coli* phage P1. These antirestriction proteins are delivered along with the phage DNA upon virion ejection and competitively bind restriction recognition sequences to protect the phage genome (67). Though Ocr, DarA, and DarB, as well as other characterized examples of antirestriction proteins differ in how and what restriction system they inhibit, most are encoded by small (<150 amino acids) proteins. Such small reading frames are abundant in phage genomes but are often recalcitrant to predictive sequence analyses due to their size and limited representation in sequence databases (68). Recent phage-bacteria coevolution studies have discovered that some of these cryptic proteins function specifically in antiphage defense (69, 70).

EF_B0059 is classified as a TIV-RE based on the presence of DUF262 and DUF1524 domains, both of which are found in other TIV-REs such as GmrSD from *E. coli* and SspE from *Vibrio cyclitrophicus* (20, 47). Bioinformatic analyses suggest that the DUF262 is responsible for NTPase activity, while DUF1524 is responsible for DNA cleavage (47). Supporting these bioinformatic results, single amino acid mutation of the DUF262 in SspE ablates its NTPase

activity, while single amino acid mutation of the DUF1524 of SspE impairs DNA cleavage (20). EF_B0059 contains a DUF262 and a DUF1524, and a single amino acid substitution of a predicted catalytic residue for each of these domains blocks the toxicity of the protein when expressed in *E. coli* (Fig. 2E). Unfortunately, EF_B0059 has proven to be very unstable during protein purification, thereby preventing further biochemical characterization of the enzyme. Therefore, we cannot entirely rule out that EF_B0059 functions differently from that of known TIV-REs in its capacity to restrict phi47 infection. However, based on its compelling structural and sequence similarity to well-characterized TIV-REs, we consider it highly likely that EF_B0059 is also a bona fide TIV-RE.

Although EF_B0058 is not essential for protection against phi47, our finding that EF_B0058 and EF_B0059 are co-transcribed (Fig. 2F) suggests that these two genes have co-evolved. Sequence analysis of EF_B0058 identifies homology to serine recombinases, which are important mediators of genotypic diversity and population-level fitness in bacteria (71). Recent reports have shown that serine recombinase genes are commonly found in phage-defense islands (14). Though not yet known to contribute to mobilization of antiphage defense systems directly, these recombinases may contribute to the diversification of defense islands through homologous recombination.

We hypothesize that ArfA may mimic DNA due to its negative surface charge. While the DNA modification of phi47 remains unknown, we hypothesize that the single amino acid mutation in ArfA may more closely mimic the modified DNA of the phage. Indeed, we demonstrated that mutation of this key phenylalanine residue significantly alters the binding affinity between ArfA and EF_B0059, lending support to a model whereby ArfA physically blocks the ability of EF_B0059 to recognize DNA. In support of a single amino acid mutation conferring differential activity of ArfA, the unrelated Ocr anti-restriction protein of bacteriophage T7 requires few amino acid mutations to alter its inhibitory activity towards different restriction systems (60).

ArfA appears to be unique to phages that infect enterococci and other lactic acid bacteria. Only a handful of proteins that function as DNA mimics have been characterized, but their structural diversity is vast (72). It is possible that many phages carry DNA mimetic proteins, but their sequence and structural diversity makes it difficult to identify them through traditional bioinformatic methods. The N-terminal domain of ArfA possesses predicted structural similarity to SH3-like domains, which are known to facilitate protein-protein interactions (58, 59). Interestingly, sequence divergence among ArfA homologs appears to localize at the N-terminus of the protein, which is the same region where leucine 32 is located. We suspect that the diversification of this domain supports the capacity of ArfA to bind and inactivate diverse TIV-REs.

In comparison to the discovery and characterization of novel phage-defense systems, investigations into how phages escape such antiphage defense systems are limited. In this study, we show that phages that infect *E. faecalis* leverage the small open reading frame *arfA* to overcome the activity of type IV restriction systems. The ArfA protein is versatile in that its N-terminus evolves amino acid substitutions that drive its binding and subsequent inactivation of TIV-REs from diverse bacteria. Thus, adaptive evolution likely strongly favors amino acid modifications in small phage proteins like ArfA to rapidly accommodate phage infection of novel bacterial hosts. Studying the countermeasures used by phages to overcome antiphage defenses will provide important knowledge that can be applied to development of sustainable phage therapeutics.

METHODS

Bacterial strains, bacteriophages, and growth conditions.

All bacterial and bacteriophage strains used in this study can be found in Table S1. *E. faecalis* strains were grown with aeration in Brain Heart Infusion (BHI, Becton Dickinson) broth or on BHI agar at 37°C. When necessary, cultures were supplemented with 15 µg/mL chloramphenicol, 20 µg/ml erythromycin, or 500 µg/mL kanamycin. For induction of the CRISPRi plasmids, cells were grown with 50 ng/mL nisin (Sigma-Aldrich). Phage plaque assays were performed in Todd-Hewitt broth (THB, Becton Dickinson) agar supplemented with 10 mM $MgSO_4$ as described elsewhere (30). To generate strains of *E. faecalis* carrying pTEF2 and its derivatives, we performed pheromone responsive plasmid matings. V19 pTEF2 and derivatives were selected with 7.5 µg/mL vancomycin and 200 µg/mL spectinomycin. JH2-2 pTEF2 and derivatives was selected with 50 µg/mL rifampicin and 200 µg/mL spectinomycin. The construction of EF_B0058 and EF_B0059 mutant strains of *E. faecalis* followed a previously published protocol for allelic exchange (73). Primers used to generate deletion constructs that were cloned into pLT06 can be found in Table S1. *Escherichia coli* and *Escherichia fergusonii* were grown in Lennox lysogeny broth (LB, Fisher) with aeration or on LB agar at 37°C. When appropriate, cultures were supplemented with 15 µg/mL chloramphenicol, 20 µg/ml erythromycin, 50 µg/mL kanamycin, 200 µg/mL trimethoprim, 15 µg/mL gentamicin, 0.5 mM IPTG, and 0.2% w/v L-rhamnose. *Clostridium sporogenes* and *Leuconostoc mesenteroides* were grown on BHI agar supplemented 0.5 g/L L-cysteine, 10 mg/L hemin, and 1 mg/L vitamin K at 37°C in an anerobic chamber.

Plasmid construction

A detailed list of the primers and plasmids used in this study can be found in Table S1. For DNA amplification by PCR*, E. faecalis, E fergusonii, L. mesenteroides, C. sporogenes,* and phi47 genomic DNA was purified using a ZymoBIOMICS DNA Miniprep Kit (Zymo Research) or a previously published protocol for phenol/chloroform extraction (30). PCR reactions used to

create DNA fragments for allelic exchange were performed using KOD Hot Start DNA Polymerase (EMD Millipore) and cloned into pLT06 (73). phi47 *orf65* and its derivatives were PCR amplified using Q5 master mix (New England Biolabs) and cloned into pLZ12A, a derivative of the shuttle vector pLZ12 carrying the *bacA* promoter (41). CRISPRi sgRNA pGCP123 plasmids were designed and cloned following previously published protocols (46). Plasmids were transformed into *E. faecalis* by electroporation. Briefly, *E. faecalis* was grown in BHI broth to an OD_{600} of 0.3. The cells were washed once with ice-cold 10% glycerol and resuspended in 500 µl of lysozyme solution (30 µg/ml lysozyme, 20% sucrose, 10 mM EDTA, 50 mM NaCl and 10 mM Tris-HCl, pH 8.0) and incubated at 37ºC for 20 min. The cells were washed four times with 500 µl of ice-cold electroporation buffer (500 mM sucrose and 10% glycerol). Cell pellets were resuspended in 250 µl of ice-cold electroporation buffer and 0.5 – 1.0 µg of plasmid DNA was electroporated into 50 µl of the *E. faecalis* suspension using a 0.2 mm cuvette at 2.5k V, 200 Ω and 25 µF. Plasmids used for heterologous expression in *E. coli* include pSCrhaB2-CV, and pPSV39-CV. All expression plasmids were constructed using standard restriction enzyme-based cloning procedures. Reagents used for cloning, including restriction enzymes, T4 DNA ligase, and Phusion DNA polymerase were obtained from New England Biolabs. Plasmids were transformed into chemically competent *E. coli* by heat-shock and transformants were subsequently isolated by selection with the appropriate antibiotics.

Genomic comparisons of *E. faecalis* strains

The chromosomes of *E. faecalis* SF28073 and V583 were obtained from NCBI and aligned using the MAUVE multiple genome alignment tool (74). To compare plasmid sequences between *E. faecalis* strains, sequences of each plasmid were obtained from NCBI and aligned using the clinker alignment tool (75).

Pheromone responsive plasmid mating

For pheromone responsive plasmid conjugation, 150 µL of overnight *E. faecalis* cultures were subcultured into 5 mL of BHI broth and grown for 90 minutes with aeration at 37°C. Donor and recipient bacteria were mixed at a 1:1 ratio in a volume of 1 mL and applied to a 0.45-micron filter. The filter was removed from the housing and placed on a BHI agar plate with the bacteria side of the filter facing up. These plates were Incubated overnight at 37°C. The following day, the filter was removed from the plate and placed in 5 mL of sterile PBS and vortexed to dislodge the bacteria from the filter. Serially diluted bacteria were plated on BHI agar containing antibiotics to select for recipient cells carrying the plasmid and were grown at 37°C for no more than 48 hrs. Potential transconjugants were screened via colony PCR to confirm the presence of the plasmid. To generate *E. faecalis* V19 pTEF2 and JH2-2 pTEF2 the donor was *E. faecalis* OG1RF pTEF2-spec^{R} (41). To generate *E. faecalis* V19 pTEF1, *E. faecalis* OG1SSp pTEF1 was used as the donor. Transconjugants were selected on BHI agar with antibiotics as described above.

Growth curves

For broth culture infections of *E. faecalis* with phi47, 15 mL of THB broth was inoculated with *E. faecalis* and grown to an OD_{600} of 0.3. Cultures were infected with phi47 at a multiplicity of infection of either 1 or 10, as indicted, and supplemented with 10 mM $MgSO_4$. Cultures were incubated at room temperature for 5 minutes, then moved to 37°C with aeration. Phage production was quantified by removing 100 µL of the culture, extracting with 33.3 µL of chloroform, and quantifying the number of phages using plaque assays (39). For the *E. coli* growth curves, overnight cultures containing the indicated plasmids were diluted 1:100 into LB

broth supplemented with 200 µg/mL trimethoprim and 15 µg/mL gentamicin. For each culture, 200 µL was seeded into a 96-well plate in triplicate. Growth was measured at 15-minute intervals until an OD_{600} of 0.4 was reached, upon which protein expression was induced by the addition of either 0.2% L-rhamnose or 0.2% L-rhamnose and 0.5 mM IPTG. For the infection of *E. coli* cells expressing BrxU and Orf65 with coliphage, overnight cultures were diluted 1:100 in LB and grown to an OD_{600} of 0.5. Expression of Orf65 and/or BrxU was induced by the addition 0.5 mM IPTG and 0.2% L-rhamnose, respectively. After 30 minutes, 500 µL of *E. coli* was mixed with 5 mL of semi-solid LB (0.75% w/v agar) supplemented with 0.5 mM IPTG and/or 0.2% L-rhamnose and poured onto an 1.5% w/v LB agar plate. The agar overlay was allowed to dry and 5 µL of serially diluted coliphages were spotted on top. After overnight incubation at 37 °C, the plaques were quantified and compared between inducing conditions.

Reverse transcription-PCR

cDNA was generated from 1 µg of RNA using qScript cDNA SuperMix (QuantaBio) and the cDNA was purified using a QIAquick PCR Purification Kit (Qiagen). 2 µL of cDNA was used in a PCR reaction with primers specific to EF_B0058 and EF_B0059 (Table S1). The resulting PCR products were run on a 1% agarose gel to visualize PCR bands.

Phage adsorption assay

E. faecalis cultures grown in BHI were pelleted at 3220 x *g* for 10 minutes and resuspended to 10^8 CFU/mL in SM-plus buffer (100 mM NaCl, 50 mM Tris-HCl, 8 mM $MgSO_4$, 5 mM $CaCl_2$ [pH 7.4]). Phages were added at an MOI of 0.1 and incubated at room-temperature without agitation for 10 minutes. The bacteria-phage suspensions were centrifuged at 24,000 x *g* for 1

minute and the supernatant was collected to determine the number of unbound phages using a plaque assay. SM-plus buffer supplemented with phage only was used as a negative control.

Western blotting

To analyze the expression of EF_B0059, its active site mutants, and Orf65, 5 mL cultures of *E. coli* containing the indicated plasmids were grown to an OD_{600} of 0.5, upon which protein expression was induced by the addition of 0.2% L-rhamnose and 0.5 mM IPTG. The cells were pelleted by centrifugation at 7,800 x *g* after 30 minutes of protein expression. Cell pellets were resuspended in 50 µL of PBS and mixed 1:1 with Laemmli buffer and boiled at 95°C for 10 minutes. Samples were centrifuged at 16,000 x *g* and 5 µL was loaded onto a 10% SDS PAGE gel. The gel was run for 15 minutes at 95 V, followed by 40 minutes at 195 V, and total protein was wet transferred to a nitrocellulose membrane using a mini–Trans-Blot electrophoretic system. After the transfer, the blot was blocked in TBS-T supplemented with 5% w/v non-fat milk, shaking gently at room temperature for 1 hour. The blot was washed three times with TBS-T and primary antibody (anti-VSV-G or anti-FLAG) was added to the blot at a 1:5000 dilution followed by an overnight incubation shaking gently at 4 °C. The blot was washed three times with TBS-T, followed by a 1-hour incubation with secondary antibody (anti-rabbit HRP conjugate). After three more washes with TBS-T, the blot was developed by the addition of ECL substrate and chemiluminescence was visualized using a ChemiDoc instrument.

CRISPRi screening

Using previously described CRISPRi constructs for *E. faecalis* (46), sgRNA oligonucleotides were designed against pTEF2 genes and ordered from Twist Bioscience. All sgRNA oligonucleotides used can be found in Table S1. *E. faecalis* V19 pTEF2 with CRISPRi and

sgRNA plasmids were cultured overnight in BHI containing 200 µg/mL kanamycin, 50 µg/mL erythromycin, and 50 ng/mL nisin. Overnight cultures were diluted to an OD_{600} of 0.1 in SM-plus buffer. 6 µL of 10-fold serial dilutions were spotted on THB agar plates supplemented with 10mM $MgSO_4$, 200 µg/mL kanamycin, 50 µg/mL erythromycin, and 50 ng/mL nisin with and without $1x10^7$ PFU/mL of phi47 embedded in the agar. Plates were incubated at 37°C for 48 hours and bacteria were enumerated. Relative viability was calculated by dividing the CFU of cells grown in the presence of phi47 by the CFU grown in the absence of phi47.

Structural modeling and comparisons

Protein structures were modelled with Colabfold (V.1.5.2) using Google Collaboratory. Predictions were run using the default parameters (56). The resulting structures were visualized, and electrostatic surface potential was mapped using ChimeraX (76). Structural comparisons and RMSD calculations were performed using the DALI webserver (77).

Isolation of *E. coli* bacteriophage from wastewater

Bacteriophages were isolated from wastewater samples as previously described with minor alterations (51). In brief, 5 mL of wastewater was centrifuged at 9,000 x *g* and then filtered through a 0.22 µM filter. The cleared wastewater was mixed with 5 mL of LB and inoculated with 500 µL of an overnight *E. coli* culture. After a 24-hour incubation shaking at 37°C, 2 mL aliquots were removed from cultures that showed evidence of phage propagation (complete cell lysis), and centrifuged at 12,000 x *g*. The supernatant was filtered through a 0.22 µM filter to remove any remaining bacterial cells. The filtered supernatant was serially diluted in SM-plus buffer from which 10 µL was added to 500 µL of an overnight *E. coli* culture. This phage-bacterial mixture was then added to 5 mL of semi-solid LB (0.75% w/v agar), mixed gently, and overlayed onto an

LB agar plate. After an overnight incubation, the resulting plaques were isolated. Agar plugs of an individual plaque was used to inoculate a culture of *E. coli* grown to mid-log phase as determined by OD_{600} measurements. Upon lysis of the *E. coli* culture, the resulting phages were purified as described above. The above infection protocol was repeated until a uniform plaque morphology was obtained.

Sequencing and genomic analysis of pTEF2 escape phi47 isolates

phi47 genomic DNA was sequenced using the Illumina NextSeq 2000 platform to 300 Mbp depth at SeqCenter (Pittsburgh, PA). The resulting reads were mapped to the phi47 genome (NCBI accession ON086985) and SNPs were identified using CLC Genomics Workbench v20 (Qiagen) with a minimum coverage of 15, a minimum frequency of 30%, and ploidy of 0. The DNA sequencing reads can be found at the European Nucleotide Archive under project accession PRJEB68205.

Co-immunoprecipitation assays

To probe the interaction between Orf65 and a given TIV-RE, 50 mL cultures of *E. coli* were grown to an OD_{600} of 0.5 upon which expression of FLAG-tagged TIV-RE and VSV-G-tagged Orf65 were induced with the addition 0.2% L-rhamnose and 0.5 mM IPTG, respectively. After 30 minutes the cells were pelleted and resuspended in 2 mL of lysis buffer (150 mM NaCl, 20 mM Tris-HCl pH 7.5) and lysed by sonication. The cell lysates were cleared by centrifugation at 16,000 x *g* for 30 minutes at 4 °C. Cleared cell lysates were incubated with 50 µL of anti-FLAG agarose beads for 2 hours at 4 °C using a tube rotator. The beads were washed three times with 10 mL of lysis buffer and bound protein was eluted by boiling in 50 µL of Laemmli buffer. 5

μL of the elution was subjected to SDS-PAGE and western blotting as described above using anti-FLAG and anti-VSV-G as the primary antibodies.

ACKNOWLEDGEMENTS

We would like to thank Dr. Michael Gilmore for providing *E. faecalis* OG1RF pTEF2-spec and *E. faecalis* OG1SSp pTEF1, Dr. Katrine Whiteson for sharing phage SDS2, Dr. Kimberly Kline for providing CRISPRi genetic tools, and Dr. Michael Surette for sharing *Clostridium sporogenes* and *Leuconostoc mesenteroides* strains. We also thank Dr. Lindsey Marmont for her constructive feedback on the manuscript.

FUNDING

This work was support by National Institutes of Health grants R01AI141479 (B.A.D.), T32AI052066 (C.N.J.), and F31AI157050 (C.N.J.), the National Science Foundation Graduate Research Fellowship Program (S.E.A.), the Burroughs Welcome Fund Investigators in the Pathogenesis of Infectious Disease Award (J.C.W.), and a Canada Research Chair in Molecular Microbiology (J.C.W.)

<u>FIGURE LEGENDS</u>

Figure 1. **The pheromone responsive plasmid pTEF2 is sufficient to inhibit phi47 replication. (A)** Capacity of phage phi47 to form plaques measured by PFU/mL on the indicated *E. faecalis* strains. **(B)** PFU/mL produced upon phi47 infection of indicated *E. faecalis* strains over 80 minutes. All strains were infected with an equivalent MOI of 1.0.

Figure 2. *EF_B0059* encodes a putative type IV restriction that prevents infection by phi47. (A) Sequence alignments between the pheromone responsive plasmids pTEF2 and pCF10. Genes highlighted in yellow indicate a sequence identify greater than 95%. **(B)** Capacity of phage phi47 to form plaques measured by PFU/mL on the indicated *E. faecalis* strains. **(C)** Relative viability of *E. faecalis* V19 pTEF2 cells upon transcription knock-down of the indicated pTEF2 encoded genes of interested using CRISPR interference. Relative viability was determined by comparing the growth of each strain in the presence and absence of phi47. Statistical significance determined by ANOVA with multiple corrections, *p=0.0004. **(D)** and **(E)** Outcome of phi47 infections measured by PFU/mL in *E. faecalis* strains V583 (D) and V19 (E) in which the genes encoding EF_B0058 or EF_B0059 on pTEF2 are deleted. **(F)** Schematic of the EF_B0058 and EF_B0059 genes. **(G)** Reverse transcription-PCR analysis of the EF_B0058 and EF_B0059 mRNA transcript in *E. faecalis* V19 with or without pTEF2. Primer sets used to probe the structure of the EF_B0058-EF_B0059 transcriptional operon are shown in red (EF_B0058 specific), green (intergenic) and blue (EF_B0059 specific). **(H)** Growth curves of *E. coli* expressing EF_B0059, the indicated active site mutants, or empty vector. Arrow indicates when protein expression was induced. **(I)** Western blot of VSV-G-tagged EF_B0059 in *E. coli* strains from (H), 30 minutes post-induction. A non-specific band from the PAGE of these samples stained with Coomassie Brilliant Blue is used as a loading control (load).

Figure 3. A mutation in the phage protein Orf65 prevents EF_B0059-dependent restriction of phi47. (A) Gene schematic of the genomic loci of *orf65* in the phi47 genome. **(B)** Capacity of phi47 to form plaques measured by PFU/mL on *E. faecalis* strain V19 or V19 carrying pTEF2 and co-expressing Orf65 or Orf65^{L32F}. **(C)** Ribbon representation of the predicted structure of Orf65 as generated using Alphafold2. The structure is colored according to the predicted local

distance difference test (pLDDT). The distribution of the acidic residues throughout the structure is also shown. **(D)** The predicted amino acid surface electrostatic potential of Orf65. **(E)** Growth curves of *E. coli* expressing EF_B0059 and either Orf65 or Orf65^{L32F}, or empty vector. The arrow indicates when protein expression was induced. **(F)** Western blot of VSV-G-tagged EF_B0059 and Orf65/Orf65^{L32F} in *E. coli* strains from (E) 30 minutes post-induction. A non-specific band from the PAGE of these samples stained with Coomassie Brilliant Blue is used as a loading control (load). **(G)** Western blot analysis of the Co-immunoprecipitation of VSV-G-tagged Orf65 or Orf65^{L32F} with FLAG-tagged EF_B0059. Tagged proteins were co-expressed in *E. coli* for 30 minutes upon which cells were lysed and FLAG-EF_B0059 was precipitated using anti-FLAG antibody conjugated to agarose beads.

Figure 4. Wildtype Orf65 inactivates distally related type IV restriction enzymes. (A) Multiple sequence alignment of residues 25-42 from Orf65 homologs identified in the genomes of 9 closely related enterococcal phages. The residues are colored according to their percent similarity at that site. **(B)** Growth curves of *E. coli* expressing GC1503 and either Orf65 or Orf65^{L32F}, or empty vector. Arrow indicates when protein expression was induced. **(C)** Western blot analysis of the Co-immunoprecipitation of VSV-G-tagged Orf65 or Orf65^{L32F} with FLAG-tagged GC1503. Tagged proteins were co-expressed in *E. coli* for 30 minutes upon which cells were lysed and FLAG-tagged EF_B0059 was precipitated using anti-FLAG antibody conjugated to agarose beads. **(D)** Outcome of coliphage infection measured by PFU/mL in *E. coli* strain XL-1 blue co-expressing BrxU and either Orf65 or Orf65^{L32F}. **(E)** Outcome of Co-immunoprecipitation as in (C) but with FLAG-tagged BrxU.

Figure S1. Genomic comparisons of *E. faecalis* strains V583 and SF28073. (A) Whole genome alignments of alignments of *E. faecalis* V583 and SF28073 chromosomes **(B)** Sequence alignments between plasmids from *E. faecalis* V583 (pTEF1, pTEF2, pTEF3) and *E. faecalis* SF28073 (pSF1, pSF2, pSF3).

Figure S2. pTEF2 prevents assembly of intracellular phage particles in an abortive infection-independent manner. (A) Growth curves of the indicated *E. faecalis* strains infected with Phi47 at an MOI of 10 The growth *E. faecalis* strain V19 containing pTEF2 was measured with and without (uninfected) the addition of phi47. (**B)** Percent of phi47 adsorbed to *E. faecalis* strains V583, V19, V19 pTEF2, and OG1RF (negative control).

Figure S3. The predicted structure of EF_B0059 resembles GmrSD-like type IV restriction enzymes. (A) Ribbon representation of the predicted structure of EF_B0059 generated using Alphafold2. The predicted local distance difference tests (pLDDT) per position is mapped onto the model. Purple corresponds to a more confident prediction at that position. The N-terminal DUF262 and C-terminal DUF1524 domains, and the residues that define each active site are indicated. **(B)** The predicted alignment error (Å) of all residues against all residues for the model in (A). Lower error (blue) corresponds to a well-defined relative position for a given residue pair.

Figure S4. The L32F mutation in Orf65 is essential for overcoming restriction by EF_B0059. (A) Outcome of either wildtype of evolved phi47 infections measured by PFU/mL of the *E. faecalis* strain V19 with or without pTEF2. **(B)** The predicted alignment error (Å) of all residues against all residues for the structural model in (Fig. 3C). Lower error (blue) corresponds to a well-defined relative position for a given residue pair. **(C)** Anti-FLAG

immunoprecipitation of VSV-G tagged Orf65 or Orf65^{L32F} expressed in the absence of EF_B0059-FLAG, detected by Western blot. **(D)** Growth curves of *E. coli* co-expressing EF_B0059 and Orf65 or the indicated Orf65 mutant. **(E)** Anti-FLAG immunoprecipitation of VSV-G tagged Orf65, or the indicated L32 mutant.

Figure S5. GC1503, but not GC874, is toxic to *E. coli* (A) Growth curves of *E. coli* expressing the indicated Orf65 variants. Orf65^{SDS2} refers to the Orf65 homolog from the enterococcus phage SDS2. **(B)** Growth curves of *E. coli* expressing either EF_B0059, GC1503, GC874, or an empty vector control. Arrow indicates when protein expression was induced. **(C)** Western blot of VSV-G-tagged EF_B0059 and Orf65 or Orf65^{L32F} in *E. coli* strains 30 minutes post-induction. A non-specific band from the PAGE of these samples stained with Coomassie Brilliant Blue is used as a loading control (load). **(D)** Growth curves of *E. coli* co-expressing GC1503 and the indicated ORf65 mutant. Arrow indicates when protein expression was induced.

Figure S6. GC1503 and GC874 are predicted to be structurally similar to EF_B0059. **(A)** Structural alignment of the predicted GC1503 (grey) and GC874 (red) models with that of EF_B0059 (blue). Domains corresponding to the N-terminal DUF262 and C-terminal DUF1524 are highlighted, along with the sequences corresponding to the conserved catalytic resides for each structure in these domains. The alignment statistics, including the sequence identify and Cα root mean squared deviations (rmsd) are also indicated. **(B)** Structural model of GC874 (upper) coloured according to the per position predicted local distance difference test (pLDDT) and the predicted alignment error (Å) plot. **(C)** Structural model of GC1503 (upper) coloured according to the per position predicted local distance difference test (pLDDT) and the predicted alignment error (Å) plot.

REFERENCES

1. Donskey CJ, Chowdhry TK, Hecker MT, Hoyen CK, Hanrahan JA, Hujer AM, Hutton-Thomas RA, Whalen CC, Bonomo RA, Rice LB. 2000. Effect of antibiotic therapy on the density of vancomycin-resistant enterococci in the stool of colonized patients. N Engl J Med 343:1925-1932. 10.1056/NEJM200012283432604

2. Ubeda C, Bucci V, Caballero S, Djukovic A, Toussaint NC, Equinda M, Lipuma L, Ling L, Gobourne A, No D, Taur Y, Jenq RR, van den Brink MRM, Xavier JB, Pamer EG. 2013. Intestinal microbiota containing *Barnesiella* species cures vancomycin-resistant *Enterococcus faecium* colonization. Infect Immun 81:965-973. 10.1128/IAI.01197-12

3. Suh GA, Lodise TP, Tamma PD, Knisely JM, Alexander J, Aslam S, Barton KD, Bizzell E, Totten KMC, Campbell JL, Chan BK, Cunningham SA, Goodman KE, Greenwood-Quaintance KE, Harris AD, Hesse S, Maresso A, Nussenblatt V, Pride D, Rybak MJ, Sund Z, van Duin D, Van Tyne D, Patel R. 2022. Considerations for the use of phage therapy in clinical practice. Antimicrob Agents Chemother 66:e0207121. 10.1128/aac.02071-21

4. Strathdee SA, Hatfull GF, Mutalik VK, Schooley RT. 2023. Phage therapy: From biological mechanisms to future directions. Cell 186:17-31. 10.1016/j.cell.2022.11.017

5. Kortright KE, Chan BK, Koff JL, Turner PE. 2019. Phage therapy: A renewed approach to combat antibiotic-resistant bacteria. Cell Host Microbe 25:219-232. 10.1016/j.chom.2019.01.014

6. Sulakvelidze A, Alavidze Z, Morris JG. 2001. Bacteriophage therapy. Antimicrob Agents Chemother 45:649-659. 10.1128/AAC.45.3.649-659.2001

7. Langdon A, Crook N, Dantas G. 2016. The effects of antibiotics on the microbiome throughout development and alternative approaches for therapeutic modulation. Genome Med 8:39. 10.1186/s13073-016-0294-z

8. Moelling K, Broecker F, Willy C. 2018. A wake-up call: We need phage therapy now. Viruses 10:688. 10.3390/v10120688

9. Brives C, Pourraz J. 2020. Phage therapy as a potential solution in the fight against AMR: obstacles and possible futures. Palgrave Communications 6:1-11. 10.1057/s41599-020-0478-4

10. Cook R, Brown N, Redgwell T, Rihtman B, Barnes M, Clokie M, Stekel DJ, Hobman J, Jones MA, Millard A. 2021. INfrastructure for a PHAge REference Database: Identification of large-scale biases in the current collection of cultured phage genomes. Phage (New Rochelle) 2:214-223. 10.1089/phage.2021.0007

11. Ofir G, Sorek R. 2018. Contemporary phage biology: From classic models to new insights. Cell 172:1260-1270. 10.1016/j.cell.2017.10.045

12. Hampton HG, Watson BNJ, Fineran PC. 2020. The arms race between bacteria and their phage foes. Nature 577:327-336. 10.1038/s41586-019-1894-8

13. Duncan-Lowey B, Kranzusch PJ. 2022. CBASS phage defense and evolution of antiviral nucleotide signaling. Curr Opin Immunol 74:156-163. 10.1016/j.coi.2022.01.002

14. Hochhauser D, Millman A, Sorek R. 2023. The defense island repertoire of the *Escherichia coli* pan-genome. PLoS Genet 19:e1010694. 10.1371/journal.pgen.1010694

15. Makarova KS, Wolf YI, Snir S, Koonin EV. 2011. Defense islands in bacterial and archaeal genomes and prediction of novel defense systems. J Bacteriol 193:6039-56. 10.1128/jb.05535-11

16. Doron S, Melamed S, Ofir G, Leavitt A, Lopatina A, Keren M, Amitai G, Sorek R. 2018. Systematic discovery of antiphage defense systems in the microbial pangenome. Science 359. 10.1126/science.aar4120

17. Brouns SJ, Jore MM, Lundgren M, Westra ER, Slijkhuis RJ, Snijders AP, Dickman MJ, Makarova KS, Koonin EV, van der Oost J. 2008. Small CRISPR RNAs guide antiviral defense in prokaryotes. Science 321:960-4. 10.1126/science.1159689

18. Mojica FJ, Diez-Villasenor C, Garcia-Martinez J, Soria E. 2005. Intervening sequences of regularly spaced prokaryotic repeats derive from foreign genetic elements. J Mol Evol 60:174-82. 10.1007/s00239-004-0046-3

19. Tock MR, Dryden DT. 2005. The biology of restriction and anti-restriction. Curr Opin Microbiol 8:466-72. 10.1016/j.mib.2005.06.003

20. Xiong X, Wu G, Wei Y, Liu L, Zhang Y, Su R, Jiang X, Li M, Gao H, Tian X, Zhang Y, Hu L, Chen S, Tang Y, Jiang S, Huang R, Li Z, Wang Y, Deng Z, Wang J, Dedon PC, Chen S, Wang L. 2020. SspABCD-SspE is a phosphorothioation-sensing bacterial defence system with broad anti-phage activities. Nat Microbiol 5:917-928. 10.1038/s41564-020-0700-6

21. Ofir G, Melamed S, Sberro H, Mukamel Z, Silverman S, Yaakov G, Doron S, Sorek R. 2018. DISARM is a widespread bacterial defence system with broad anti-phage activities. Nat Microbiol 3:90-98. 10.1038/s41564-017-0051-0

22. Goldfarb T, Sberro H, Weinstock E, Cohen O, Doron S, Charpak-Amikam Y, Afik S, Ofir G, Sorek R. 2015. BREX is a novel phage resistance system widespread in microbial genomes. EMBO J 34:169-83. 10.15252/embj.201489455

23. Pecota DC, Wood TK. 1996. Exclusion of T4 phage by the *hok*/*sok* killer locus from plasmid R1. J Bacteriol 178:2044-50. 10.1128/jb.178.7.2044-2050.1996

24. Fineran PC, Blower TR, Foulds IJ, Humphreys DP, Lilley KS, Salmond GP. 2009. The phage abortive infection system, ToxIN, functions as a protein-RNA toxin-antitoxin pair. Proc Natl Acad Sci U S A 106:894-9. 10.1073/pnas.0808832106

25. Dy RL, Przybilski R, Semeijn K, Salmond GP, Fineran PC. 2014. A widespread bacteriophage abortive infection system functions through a Type IV toxin-antitoxin mechanism. Nucleic Acids Res 42:4590-605. 10.1093/nar/gkt1419

26. Cohen D, Melamed S, Millman A, Shulman G, Oppenheimer-Shaanan Y, Kacen A, Doron S, Amitai G, Sorek R. 2019. Cyclic GMP-AMP signalling protects bacteria against viral infection. Nature 574:691-695. 10.1038/s41586-019-1605-5

27. Millman A, Bernheim A, Stokar-Avihail A, Fedorenko T, Voichek M, Leavitt A, Oppenheimer-Shaanan Y, Sorek R. 2020. Bacterial retrons function in anti-phage defense. Cell 183:1551-1561 e12. 10.1016/j.cell.2020.09.065

28. Kronheim S, Daniel-Ivad M, Duan Z, Hwang S, Wong AI, Mantel I, Nodwell JR, Maxwell KL. 2018. A chemical defence against phage infection. Nature 564:283-286. 10.1038/s41586-018-0767-x

29. Burmeister AR, Fortier A, Roush C, Lessing AJ, Bender RG, Barahman R, Grant R, Chan BK, Turner PE. 2020. Pleiotropy complicates a trade-off between phage resistance and antibiotic resistance. Proc Natl Acad Sci U S A 117:11207-11216. 10.1073/pnas.1919888117

30. Duerkop BA, Huo W, Bhardwaj P, Palmer KL, Hooper LV. 2016. Molecular basis for lytic bacteriophage resistance in enterococci. mBio 7. 10.1128/mBio.01304-16

31. Gordillo Altamirano F, Forsyth JH, Patwa R, Kostoulias X, Trim M, Subedi D, Archer SK, Morris FC, Oliveira C, Kielty L, Korneev D, O'Bryan MK, Lithgow TJ, Peleg AY, Barr JJ. 2021. Bacteriophage-resistant *Acinetobacter baumannii* are resensitized to antimicrobials. Nat Microbiol 6:157-161. 10.1038/s41564-020-00830-7

32. Eugster MR, Morax LS, Huls VJ, Huwiler SG, Leclercq A, Lecuit M, Loessner MJ. 2015. Bacteriophage predation promotes serovar diversification in *Listeria monocytogenes*. Mol Microbiol 97:33-46. 10.1111/mmi.13009

33. Canfield GS, Chatterjee A, Espinosa J, Mangalea MR, Sheriff EK, Keidan M, McBride SW, McCollister BD, Hang HC, Duerkop BA. 2021. Lytic bacteriophages facilitate antibiotic sensitization of *Enterococcus faecium*. Antimicrobial Agents and Chemotherapy 65:e00143-21, AAC.00143-21. 10.1128/AAC.00143-21

34. Paul BG, Burstein D, Castelle CJ, Handa S, Arambula D, Czornyj E, Thomas BC, Ghosh P, Miller JF, Banfield JF, Valentine DL. 2017. Retroelement-guided protein diversification abounds in vast lineages of bacteria and archaea. Nat Microbiol 2:17045. 10.1038/nmicrobiol.2017.45

35. Rusinov IS, Ershova AS, Karyagina AS, Spirin SA, Alexeevski AV. 2018. Avoidance of recognition sites of restriction-modification systems is a widespread but not universal anti-restriction strategy of prokaryotic viruses. BMC Genomics 19:885. 10.1186/s12864-018-5324-3

36. Golovenko D, Manakova E, Tamulaitiene G, Grazulis S, Siksnys V. 2009. Structural mechanisms for the 5'-CCWGG sequence recognition by the N- and C-terminal domains of EcoRII. Nucleic Acids Res 37:6613-24. 10.1093/nar/gkp699

37. Blower TR, Evans TJ, Przybilski R, Fineran PC, Salmond GP. 2012. Viral evasion of a bacterial suicide system by RNA-based molecular mimicry enables infectious altruism. PLoS Genet 8:e1003023. 10.1371/journal.pgen.1003023

38. Samson JE, Belanger M, Moineau S. 2013. Effect of the abortive infection mechanism and type III toxin/antitoxin system AbiQ on the lytic cycle of *Lactococcus lactis* phages. J Bacteriol 195:3947-56. 10.1128/JB.00296-13

39. Chatterjee A, Johnson CN, Luong P, Hullahalli K, McBride SW, Schubert AM, Palmer KL, Carlson PE, Duerkop BA. 2019. Bacteriophage resistance alters antibiotic-ediated intestinal expansion of enterococci. Infect Immun 87:e00085-19. 10.1128/IAI.00085-19

40. Furlan S, Matos RC, Kennedy SP, Doublet B, Serror P, Rigottier-Gois L. 2019. Fitness restoration of a genetically tractable *Enterococcus faecalis* V583 derivative to study decoration-related phenotypes of the enterococcal polysaccharide antigen. mSphere 4. 10.1128/mSphere.00310-19

41. Manson JM, Hancock LE, Gilmore MS. 2010. Mechanism of chromosomal transfer of Enterococcus faecalis pathogenicity island, capsule, antimicrobial resistance, and other traits. Proc Natl Acad Sci U S A 107:12269-74. 10.1073/pnas.1000139107

42. Dunny GM. 2013. Enterococcal sex pheromones: signaling, social behavior, and evolution. Annu Rev Genet 47:457-82. 10.1146/annurev-genet-111212-133449

43. Paulsen IT, Banerjei L, Myers GSA, Nelson KE, Seshadri R, Read TD, Fouts DE, Eisen JA, Gill SR, Heidelberg JF, Tettelin H, Dodson RJ, Umayam L, Brinkac L, Beanan M, Daugherty S, DeBoy RT, Durkin S, Kolonay J, Madupu R, Nelson W, Vamathevan J, Tran B, Upton J, Hansen T, Shetty J, Khouri H, Utterback T, Radune D, Ketchum KA, Dougherty BA, Fraser CM. 2003. Role of mobile DNA in the evolution of vancomycin-resistant Enterococcus faecalis. Science 299:2071-2074. 10.1126/science.1080613

44. Altschul SF, Gish W, Miller W, Myers EW, Lipman DJ. 1990. Basic local alignment search tool. J Mol Biol 215:403-410. 10.1016/S0022-2836(05)80360-2

45. Fernandez-Garcia L, Wood TK. 2023. Phage-defense systems are unlikely to cause cell suicide. Viruses 15. 10.3390/v15091795

46. Afonina I, Ong J, Chua J, Lu T, Kline KA. 2020. Multiplex CRISPRi system enables the study of stage-specific biofilm genetic requirements in *Enterococcus faecalis*. mBio 11:e01101-20. 10.1128/mBio.01101-20

47. Machnicka MA, Kaminska KH, Dunin-Horkawicz S, Bujnicki JM. 2015. Phylogenomics and sequence-structure-function relationships in the GmrSD family of Type IV restriction enzymes. BMC Bioinformatics 16:336. 10.1186/s12859-015-0773-z

48. Jablonska J, Matelska D, Steczkiewicz K, Ginalski K. 2017. Systematic classification of the His-Me finger superfamily. Nucleic Acids Res 45:11479-11494. 10.1093/nar/gkx924

49. Bair CL, Black LW. 2007. A type IV modification dependent restriction nuclease that targets glucosylated hydroxymethyl ytosine modified DNAs. J Mol Biol 366:768-778. 10.1016/j.jmb.2006.11.051

50. He X, Hull V, Thomas JA, Fu X, Gidwani S, Gupta YK, Black LW, Xu SY. 2015. Expression and purification of a single-chain Type IV restriction enzyme Eco94GmrSD and determination of its substrate preference. Sci Rep 5:9747. 10.1038/srep09747

51. Picton DM, Luyten YA, Morgan RD, Nelson A, Smith DL, Dryden DTF, Hinton JCD, Blower TR. 2021. The phage defence island of a multidrug resistant plasmid uses both BREX and type IV restriction for complementary protection from viruses. Nucleic Acids Res 49:11257-11273. 10.1093/nar/gkab906

52. Stern A, Sorek R. 2011. The phage-host arms race: shaping the evolution of microbes. Bioessays 33:43-51. 10.1002/bies.201000071

53. Rocha EP, Danchin A, Viari A. 2001. Evolutionary role of restriction/modification systems as revealed by comparative genome analysis. Genome Res 11:946-58. 10.1101/gr.gr-1531rr

54. Varadi M, Anyango S, Deshpande M, Nair S, Natassia C, Yordanova G, Yuan D, Stroe O, Wood G, Laydon A, Žídek A, Green T, Tunyasuvunakool K, Petersen S, Jumper J, Clancy E, Green R, Vora A, Lutfi M, Figurnov M, Cowie A, Hobbs N, Kohli P, Kleywegt G, Birney E, Hassabis D, Velankar S. 2021. AlphaFold protein structure database: Massively expanding the structural coverage of protein-sequence space with high-accuracy models. Nucleic Acids Res 50:D439-D444. 10.1093/nar/gkab1061

55. Jumper J, Evans R, Pritzel A, Green T, Figurnov M, Ronneberger O, Tunyasuvunakool K, Bates R, Žídek A, Potapenko A, Bridgland A, Meyer C, Kohl SAA, Ballard AJ, Cowie A, Romera-Paredes B, Nikolov S, Jain R, Adler J, Back T, Petersen S, Reiman D, Clancy E, Zielinski M, Steinegger M, Pacholska M, Berghammer T, Bodenstein S, Silver D, Vinyals O, Senior AW, Kavukcuoglu K, Kohli P, Hassabis D. 2021. Highly accurate protein structure prediction with AlphaFold. Nature 596:583-589. 10.1038/s41586-021-03819-2

56. Mirdita M, Schutze K, Moriwaki Y, Heo L, Ovchinnikov S, Steinegger M. 2022. ColabFold: making protein folding accessible to all. Nat Methods 19:679-682. 10.1038/s41592-022-01488-1

57. Holm L, Laiho A, Törönen P, Salgado M. 2023. DALI shines a light on remote homologs: One hundred discoveries. Protein Sci 32:e4519. 10.1002/pro.4519

58. Whisstock JC, Lesk AM. 1999. SH3 domains in prokaryotes. Trends Biochem Sci 24:132-133. 10.1016/s0968-0004(99)01366-3

59. Musacchio A, Wilmanns M, Saraster M. 1994. Structure and function of the SH3 domain. Prog Biophys Mol Biol 61:283-297. 10.1016/0079-6107(94)90003-5

60. Roberts GA, Stephanou AS, Kanwar N, Dawson A, Cooper LP, Chen K, Nutley M, Cooper A, Blakely GW, Dryden DTF. 2012. Exploring the DNA mimicry of the Ocr protein of phage T7. Nucleic Acids Res 40:8129-8143. 10.1093/nar/gks516

61. Walkinshaw MD, Taylor P, Sturrock SS, Atanasiu C, Berge T, Henderson RM, Edwardson JM, Dryden DTF. 2002. Structure of Ocr from bacteriophage T7, a protein that mimics B-form DNA. Mol Cell 9:187-194. 10.1016/s1097-2765(02)00435-5

62. Xu S-Y, Corvaglia AR, Chan S-H, Zheng Y, Linder P. 2011. A type IV modification-dependent restriction enzyme SauUSI from *Staphylococcus aureus* subsp. aureus USA300. Nucleic Acids Res 39:5597-5610. 10.1093/nar/gkr098

63. Goldfarb T, Sberro H, Weinstock E, Cohen O, Doron S, Charpak-Amikam Y, Afik S, Ofir G, Sorek R. 2015. BREX is a novel phage resistance system widespread in microbial genomes. EMBO J 34:169-183. 10.15252/embj.201489455

64. Krüger DH, Schroeder C, Hansen S, Rosenthal HA. 1977. Active protection by bacteriophages T3 and T7 against *E. coli* B- and K-specific restriction of their DNA. Mol Gen Genet 153:99-106. 10.1007/BF01036001

65. Bandyopadhyay PK, Studier FW, Hamilton DL, Yuan R. 1985. Inhibition of the type I restriction-modification enzymes EcoB and EcoK by the gene 0.3 protein of bacteriophage T7. J Mol Biol 182:567-578. 10.1016/0022-2836(85)90242-6

66. Kennaway CK, Obarska-Kosinska A, White JH, Tuszynska I, Cooper LP, Bujnicki JM, Trinick J, Dryden DTF. 2009. The structure of M.EcoKI Type I DNA methyltransferase with a DNA mimic antirestriction protein. Nucleic Acids Res 37:762-770. 10.1093/nar/gkn988

67. Pratt EA, Kuno S, Lehman IR. 1963. Glucosylation of the deoxyribonucleic acid in hybrids of coliphages T2 and T4. Biochim Biophys Acta 68:108-111. 10.1016/0926-6550(63)90413-4

68. Fremin BJ, Bhatt AS, Kyrpides NC. 2022. Thousands of small, novel genes predicted in global phage genomes. Cell Rep 39:110984. 10.1016/j.celrep.2022.110984

69. Millman A, Melamed S, Leavitt A, Doron S, Bernheim A, Hor J, Garb J, Bechon N, Brandis A, Lopatina A, Ofir G, Hochhauser D, Stokar-Avihail A, Tal N, Sharir S, Voichek M, Erez Z, Ferrer JLM, Dar D, Kacen A, Amitai G, Sorek R. 2022. An expanded arsenal of immune systems that protect bacteria from phages. Cell Host Microbe 30:1556-1569 e5. 10.1016/j.chom.2022.09.017

70. LeRoux M, Srikant S, Teodoro GIC, Zhang T, Littlehale ML, Doron S, Badiee M, Leung AKL, Sorek R, Laub MT. 2022. The DarTG toxin-antitoxin system provides phage defence by ADP-ribosylating viral DNA. Nat Microbiol 7:1028-1040. 10.1038/s41564-022-01153-5

71. Trzilova D, Tamayo R. 2021. Site-specific recombination - how simple DNA inversions produce complex phenotypic heterogeneity in bacterial populations. Trends Genet 37:59-72. 10.1016/j.tig.2020.09.004

72. Wang H-C, Ho C-H, Hsu K-C, Yang J-M, Wang AHJ. 2014. DNA mimic proteins: functions, structures, and bioinformatic analysis. Biochemistry 53:2865-2874. 10.1021/bi5002689

73. Thurlow LR, Thomas VC, Hancock LE. 2009. Capsular polysaccharide production in *Enterococcus faecalis* and contribution of CpsF to capsule serospecificity. J Bacteriol 191:6203-10. 10.1128/jb.00592-09

74. Darling AE, Mau B, Perna NT. 2010. progressiveMauve: multiple genome alignment with gene gain, loss and rearrangement. PLoS One 5:e11147. 10.1371/journal.pone.0011147

75. Gilchrist CLM, Chooi Y-H. 2021. clinker & clustermap.js: automatic generation of gene cluster comparison figures. Bioinformatics 37:2473-2475. 10.1093/bioinformatics/btab007

76. Goddard TD, Huang CC, Meng EC, Pettersen EF, Couch GS, Morris JH, Ferrin TE. 2018. UCSF ChimeraX: Meeting modern challenges in visualization and analysis. Protein Sci 27:14-25. 10.1002/pro.3235

77. Holm L. 2020. Using Dali for protein structure comparison. Methods Mol Biol 2112:29-42. 10.1007/978-1-0716-0270-6_3

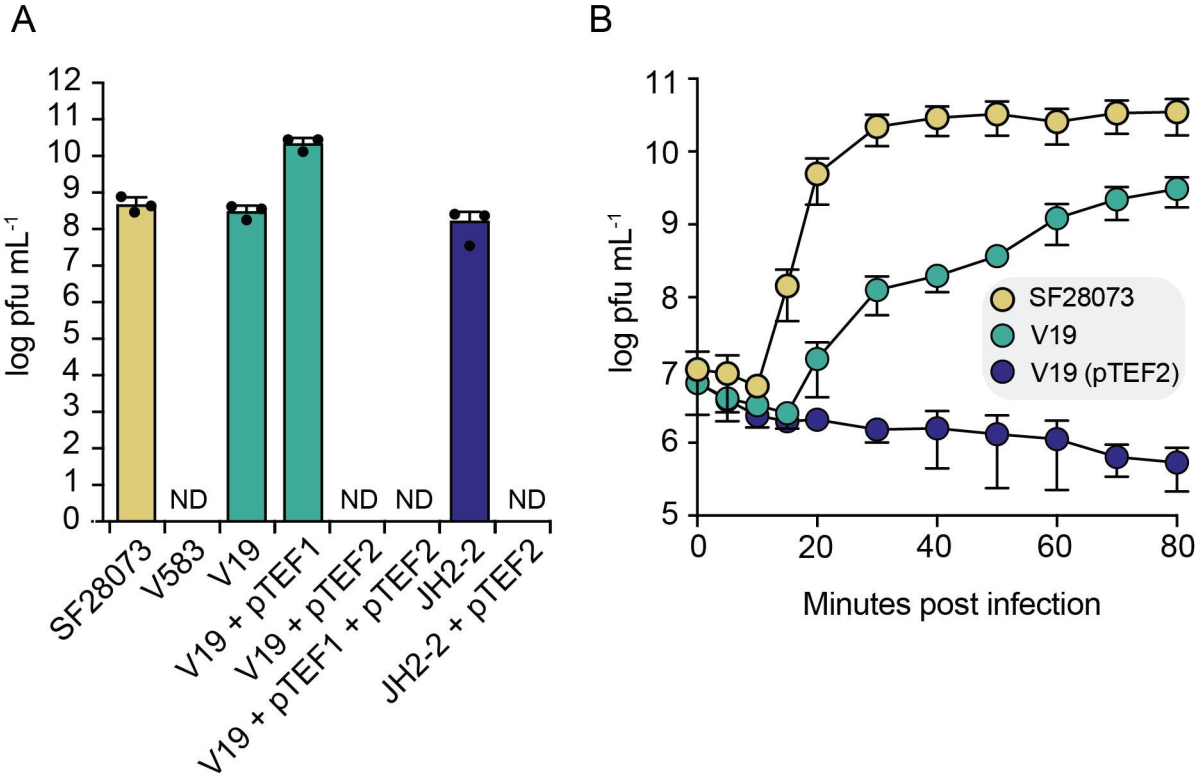
A
log pfu mL-1
12
11
10
9
8
7
6
5
4
3
2
1
0
ND
ND
ND
ND
SF28073
V583
V19
V19 + pTEF1
V19 + pTEF2
V19 + pTEF2
V19 + pTEF1 + pTEF2
JH2-2
JH2-2 + pTEF2
B
log pfu mL-1
11
10
9
8
7
6
5
0
20
40
60
80
Minutes post infection
SF28073
V19
V19 (pTEF2)

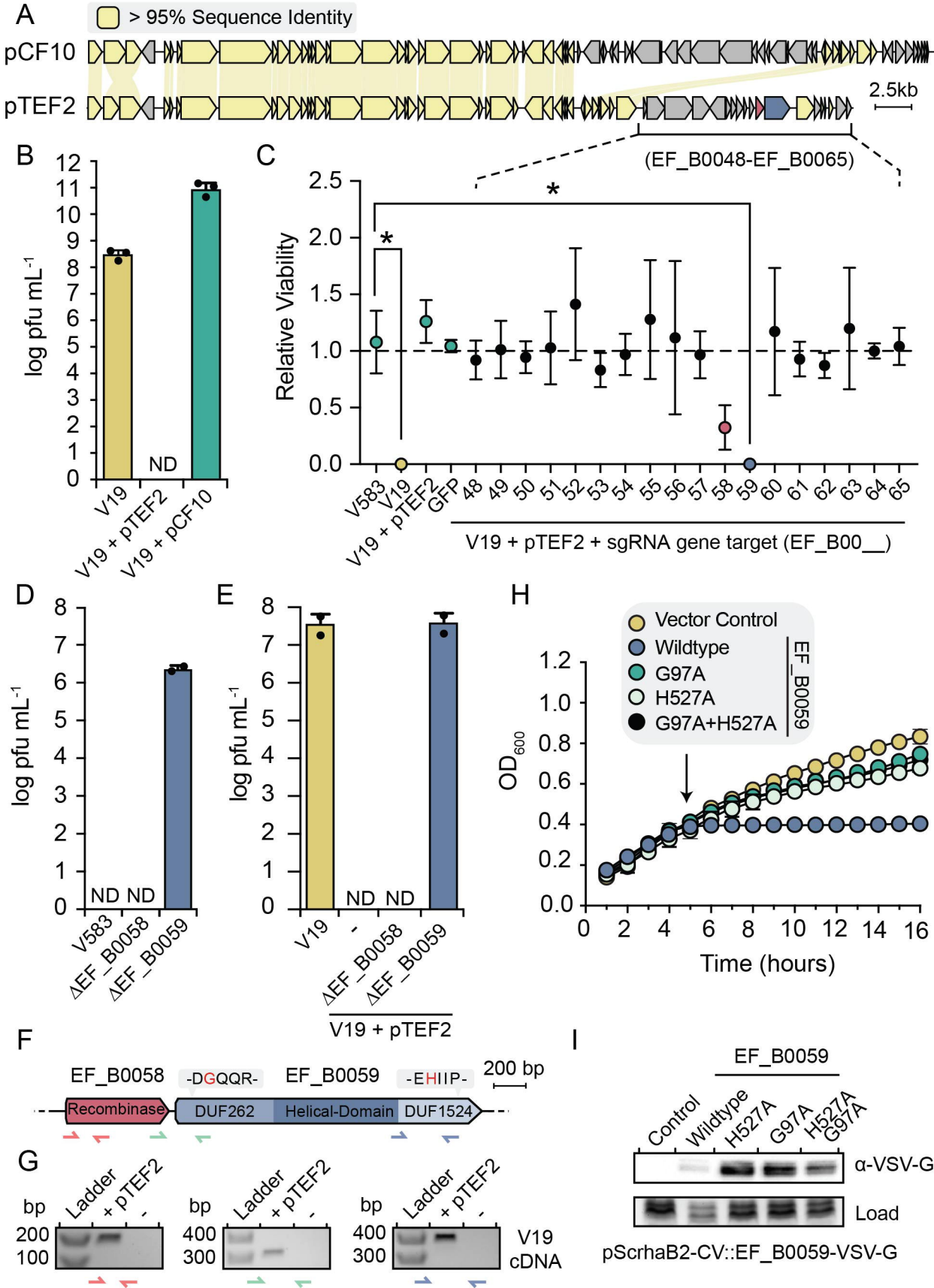
A
> 95% Sequence Identity
pCF10
pTEF2
2.5kb
B
log pfu mL-1
ND
V19
V19 + pTEF2
V19 + pCF10
C
(EF_B0048-EF_B0065)
Relative Viability
V583
V19
V19 + pTEF2
GFP
48 49 50 51 52 53 54 55 56 57 58 59 60 61 62 63 64 65
V19 + pTEF2 + sgRNA gene target (EF_B00__)
D
log pfu mL-1
ND ND
V583
ΔEF_B0058
ΔEF_B0059
E
log pfu mL-1
ND ND
V19
-
ΔEF_B0058
ΔEF_B0059
V19 + pTEF2
H
Vector Control
Wildtype
G97A
H527A
G97A+H527A
EF_B0059
OD600
Time (hours)
F
EF_B0058
-DGQQR-
EF_B0059
-EHIIP-
200 bp
Recombinase
DUF262
Helical-Domain
DUF1524
G
bp
Ladder
+ pTEF2
-
200
100
400
300
V19 cDNA
I
EF_B0059
Control
Wildtype
H527A
G97A
H527A G97A
α-VSV-G
Load
pScrhaB2-CV::EF_B0059-VSV-G

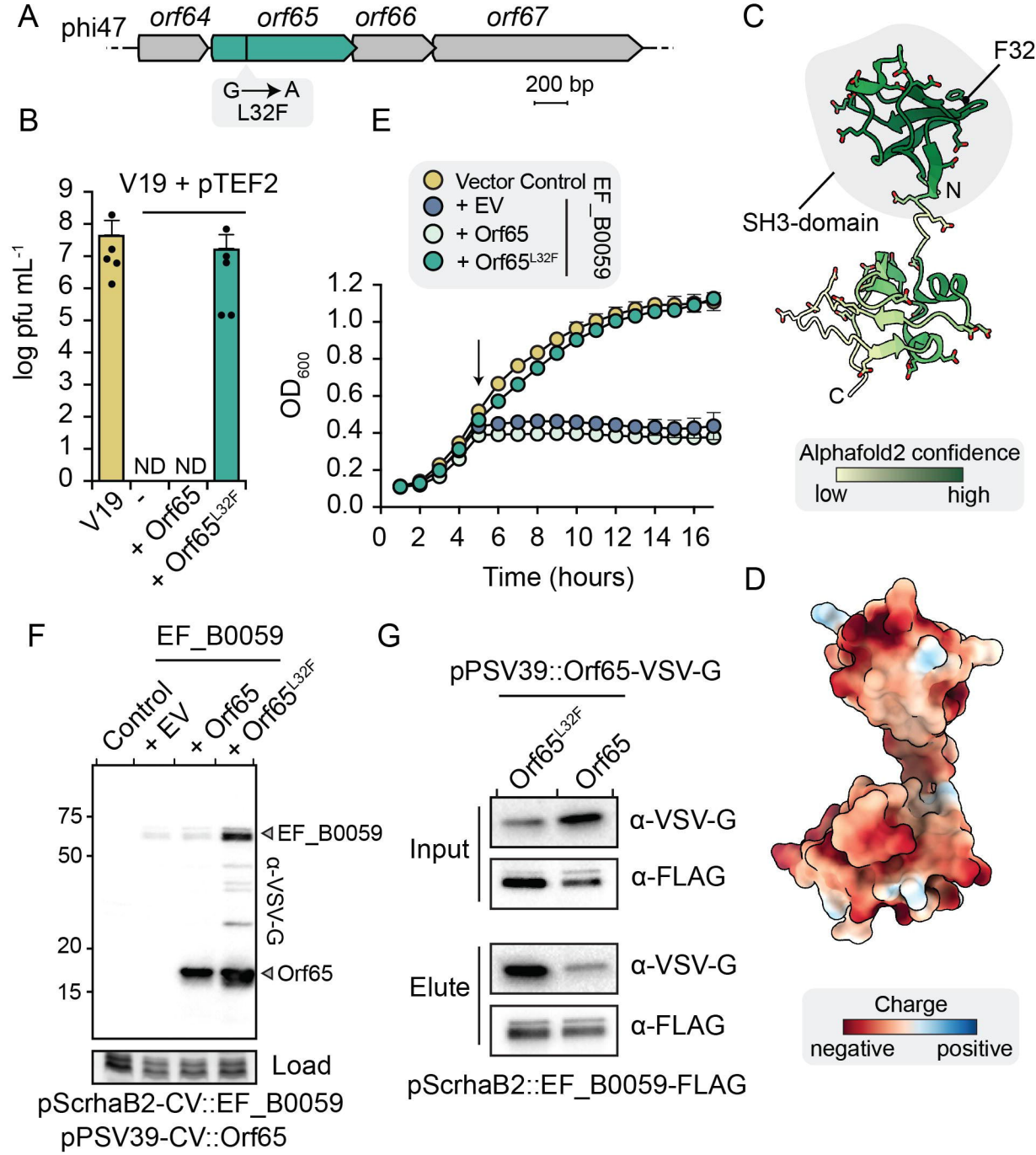
A
phi47
orf64
orf65
orf66
orf67
G → A
L32F
200 bp
B
V19 + pTEF2
log pfu mL-1
ND ND
V19
-
+ Orf65
+ Orf65L32F
C
F32
N
SH3-domain
C
Alphafold2 confidence
low
high
D
Charge
negative
positive
E
Vector Control
+ EV
+ Orf65
+ Orf65L32F
EF_B0059
OD600
Time (hours)
F
EF_B0059
Control
+ EV
+ Orf65
+ Orf65L32F
EF_B0059
α-VSV-G
Orf65
Load
pScrhaB2-CV::EF_B0059
pPSV39-CV::Orf65
G
pPSV39::Orf65-VSV-G
Orf65L32F
Orf65
Input
Elute
α-VSV-G
α-FLAG
pScrhaB2::EF_B0059-FLAG

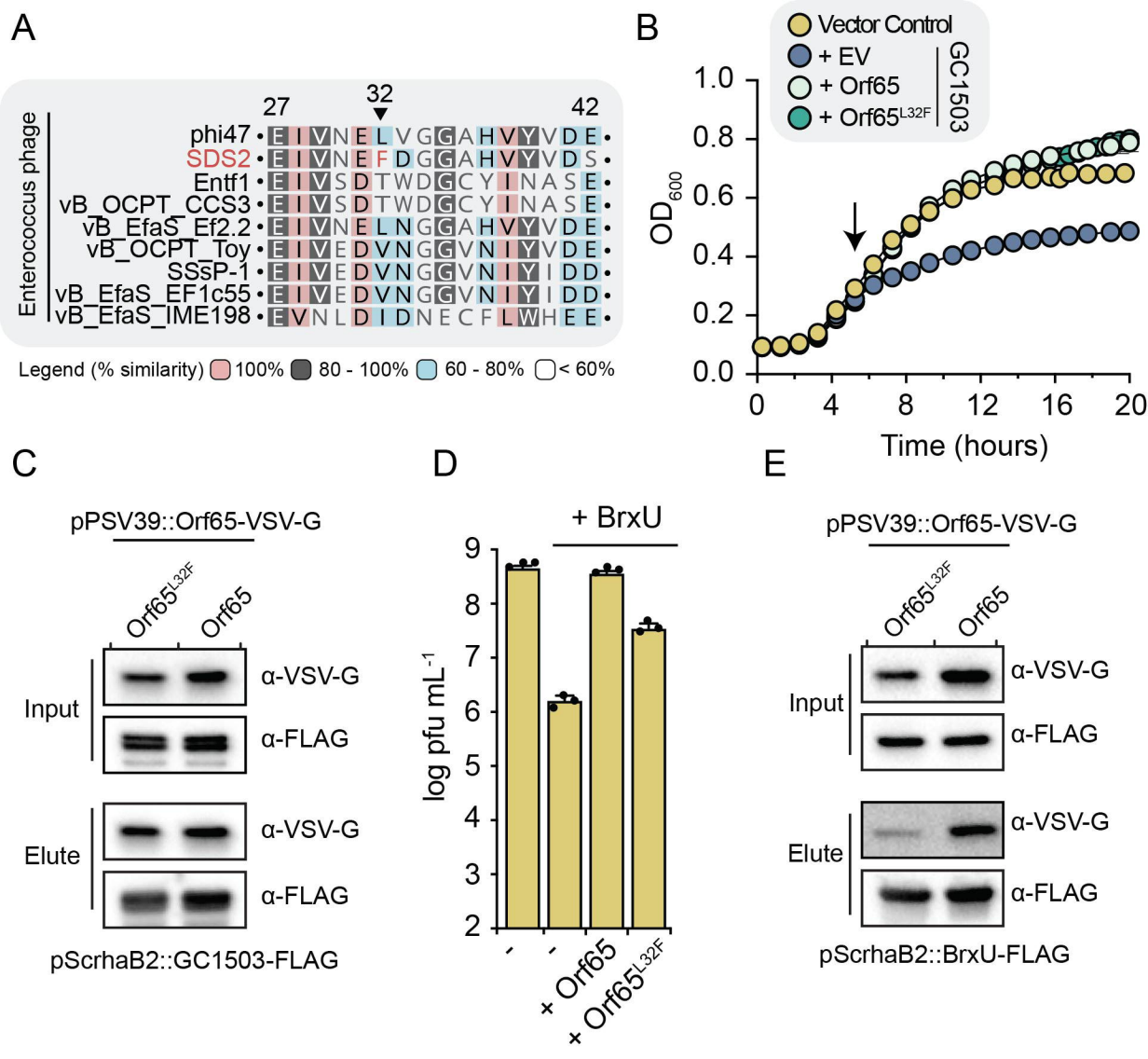
A
27
32
42
Enterococcus phage
phi47 • E I V N E L V G G A H V Y V D E •
SDS2 • E I V N E F D G G A H V Y V D S •
Entf1 • E I V S D T W D G C Y I N A S E •
vB_OCPT_CCS3 • E I V S D T W D G C Y I N A S E •
vB_EfaS_Ef2.2 • E I V N E L N G G A H V Y V D E •
vB_OCPT_Toy • E I V E D V N G G V N I Y V D E •
SSsP-1 • E I V E D V N G G V N I Y I D D •
vB_EfaS_EF1c55 • E I V E D V N G G V N I Y I D D •
vB_EfaS_IME198 • E V N L D I D N E C F L W H E E •
Legend (% similarity) 100% 80 - 100% 60 - 80% < 60%
B
Vector Control
+ EV
+ Orf65
+ Orf65L32F
GC1503
OD600
Time (hours)
C
pPSV39::Orf65-VSV-G
Orf65L32F
Orf65
Input
Elute
α-VSV-G
α-FLAG
pScrhaB2::GC1503-FLAG
D
+ BrxU
log pfu mL-1
-
-
+ Orf65
+ Orf65L32F
E
pPSV39::Orf65-VSV-G
Orf65L32F
Orf65
Input
Elute
α-VSV-G
α-FLAG
pScrhaB2::BrxU-FLAG